Do explicitly polarizable force fields give better description of biomembranes?

Hanne Antila, Batuhan Kav,* Jesper J. Madsen, Markus S. Miettinen, and O. H. Samuli Ollila

Forschungszentrum Juelich, Germany

E-mail: batuhankav@gmail.com

Abstract

With the increase of available computational capabilities, polarizable molecular dynamics force fields have gained popularity in modelling biomolecular systems. In the case of biomembranes in particular, they are expected to provide better description, eg., by capturing the varying dielectric environment across the lipid bilayer. Here, we use the framework established within the NMRlipids open science project and the related NMRlipids databank to test the commonly used polarizable lipid models, CHARMM-Drude and AMOEBA, against high fidelity experimental data and best non-polarizable models.

Introduction

In conventional molecular dynamics (MD) simulations, electrostatic interactions are described by assigning static point charges to the atoms and molecules at the beginning of the simulation as defined in the inputted model—the force field. Dynamic effects arising from molecular polarizability are traditionally not explicitly included and only considered

in an averaged fashion via force field parameterization process where parameters are obtained by fitting to macroscopic observables or to ab initio calculations. Significant efforts have been dedicated to introduce explicit polarizability into MD simulations, in the hopes of reaching a more accurate representation of the system.[1? ? –6] This effort has been motivated by the plethora of interactions where polarization is perceived to be a key contribution to correctly describing the system. These include description of water, ion hydration and ion binding to molecules, cation–π and π-π interactions.[7] These lower-level interactions also translate to the behaviour of larger-scale biological systems, such as ion channels, where ion-selectivity and ion currents may be affected by polarization,[8–11] and telomeric DNA[12] where the conformations adopted are mediated by ionic interactions.

For bilayer membrane simulation, specifically, the molecular (dielectric) environment varies dramatically while crossing the membrane from the water phase across the dipolar/charged lipid headgroup interface to the hydrophobic tail region. Therefore, including polarizability in the lipids is expected to provide more accurate description, especially in situations pertaining to membrane binding processes, membrane potential and translocation of charged biomolecules across the membrane, and the behavior of molecules residing within membranes, such as membrane proteins.[5,6,13–19]

The available lipid force fields with explicit electronic polarization include CHARMM-Drude,[13,20] AMOEBA,[14,21] and CHARMM-Fluctuating Charge (FQ).[22] The underlying strategy for including explicit polarizability differ among these models: 1) the classical Drude oscillator (CHARMM-Drude) models polarization by separating a core and a shell charge with a spring which stretches according to the environment giving the site a fluctuating dipole moment,[5] 2) the induced point dipole/multipole (AMOEBA) uses polarizable point dipoles placed on chosen sites of the molecule,[23] and 3) the electronegativity equilization (FQ) employs atomic charges that are no longer constant but can change (redistribute within the molecule) according to the electronegativities of the molecule atoms and the electric fields from the molecular environment.[24] All of these approaches result in an increasing compu-

tational cost, e.g, by introducing new types of interactions, more interactions sites, or by requiring a shorter time step in the simulations. As an alternative approach, electronic continuum correction (ECC) has been proposed as a computational efficient method to implicitly include polarizability by scaling the atom partial charges.[17,25]

Our previous efforts in benchmarking state-of-the-art non-polarizable lipid force fields have demonstrated that the quality of predictions for important membrane properties greatly vary between different force fields, particularly for lipid headgroup conformational ensembles and ion binding affinities.[26–32] The ability to capture these membrane properties correctly is important on its own but also creates the basis for the description of more complex systems: for example, ion binding affinity regulates membrane surface charge and wide variety of conformations available for lipid headgroups appears to be important for modeling realistic protein-lipid binding.[29] Therefore, such benchmark studies are urgently needed also for polarizable lipid force fields, considering the increased computational cost they come with, and most importantly, their pledge to capture a broader range of physical phenomena pertinent to enhancing our understanding of in particular polar membrane regions.

Here we assess the quality of actively developed polarizable lipid force fields, CHARMM-Drude[13,20] and AMOEBA,[14,21] using the resources and the framework from the NMRLipids open collaboration (`http://nmrlipids.blogspot.fi/`). These two force fields were selected for comparison because they are increasingly utilized in biomolecular simulations and have parameters available for several lipids for which corresponding experimental data is available in NMRlipids databank.[32] We assess the structural quality of POPC, DOPC and POPE lipid bilayer simulations against experimental NMR and small angle X-ray scattering (SAXS) data using the quality metrics defined in the NMRlipids databank.[32] Cation binding to membranes was evaluated against NMR order parameters[27] and lipid conformational dynamics is benchmarked to data from NMR spin relaxation rate experiments.[30,33] Furthermore, for each experimental benchmark we compare the results from polarizable models to those from the best performing non-polarizable simulations obtained from the NMRlipids Databank.[32]

Results and Discussion

Evaluation of lipid bilayer structural properties

To evaluate the structural properties of lipid bilayers in simulations with polarizable force fields, we simulated POPC and POPE lipid bilayers with CHARMM-Drude2017[13] and CHARMM-Drude2023[20] parameters, and POPE and DOPC bilayers with AMOEBA[14,21] parameters. These systems were selected based on simultaneous availability of force field parameters, and experimental data.[32] After the data production, simulation trajectories were added into the NMRlipids Databank and its quality metrics was used to evaluate each simulation against experiments.[32] This metric measures the quality of lipid bilayer simulations in two aspects: first, it evaluates the quality of conformational ensemble of individual lipids against C-H bond order parameters from NMR, and second, it examines consistency of membrane dimensions compared to small angle X-ray scattering (SAXS) data.[32,34] The former is divided into three parts that separately describe the average quality of headgroup, glycerol backbone and acyl chain qualities as described in the NMRlipids databank.[32] While order parameters primarily reflect lipid conformations, acyl chain order parameters are also a good proxy for membrane packing since a smaller area per lipid tends to increase the magnitude of the order parameters.[32]

Direct comparisons between simulated and experimental data are visualized in Fig 2 and the resulting quality metrics are shown in Table 1. Similarly to the non-polarizable CHARMM36 simulations, CHARMM-Drude2017 simulation predicts slightly too packed membrane with excessively negative order parameters with respect to experiments and simulations with the highest quality in the NMRlipids databank (OPLS3e).[32] However, the quality of headgroup conformations in the CHARMM-Drude2017 simulations is worse than in its non-polarizable counterpart. This is likely because headgroup and glycerol backbone parameters were optimized to reproduce absolute average values of the experimentally determined order parameters, instead of taking into account the order parameter forking

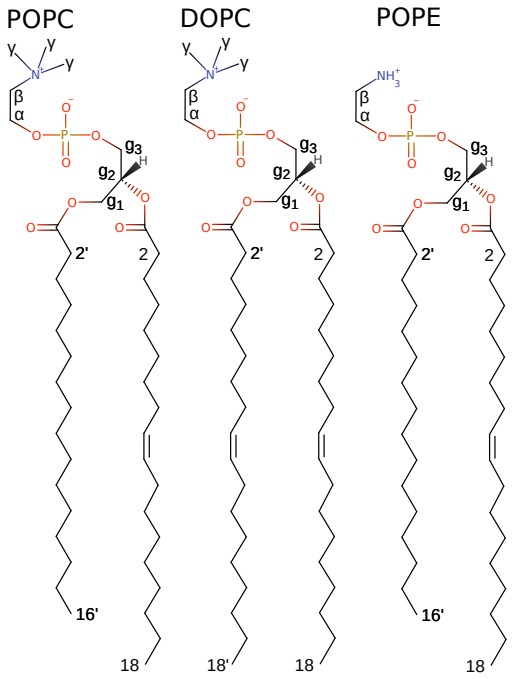

Figure 1: Molecules and atom labelling used.

(meaning measurably different order parameters for different C–H bonds at a single carbon atom) and order parameter sign.[31] A better description of the headgroup and glycerol backbone is provided by CHARMM36-Drude2023, yet its quality is still below that offered by the non-polarizable CHARMM36 parameters (see also discussion about conformational dynamics below). Also the quality of membrane packing and acyl chain order are improved in CHARMM36-Drude2023 compared to the earlier version but again, it did not perform at a quality comparable to that of the best available simulations.

AMOEBA simulations capture the headgroup and glycerol backbone order parameters reasonably well with the exception of g_1, where forking of order parameters is unacceptably large. However, experimentally observed low order parameters at double bond region in both DOPC acyl chains and *sn*-2 chain of POPE are not captured. These low order parameters signal an important mechanism through which acyl chain double bonds affect membrane properties[45] and are well reproduced in all state-of-the art MD simulation parameters.[34] Furthermore, AMOEBA parameters substantially overestimate the area per lipid in POPE simulations, leading to too disordered acyl chains. Similar issues are evident also in

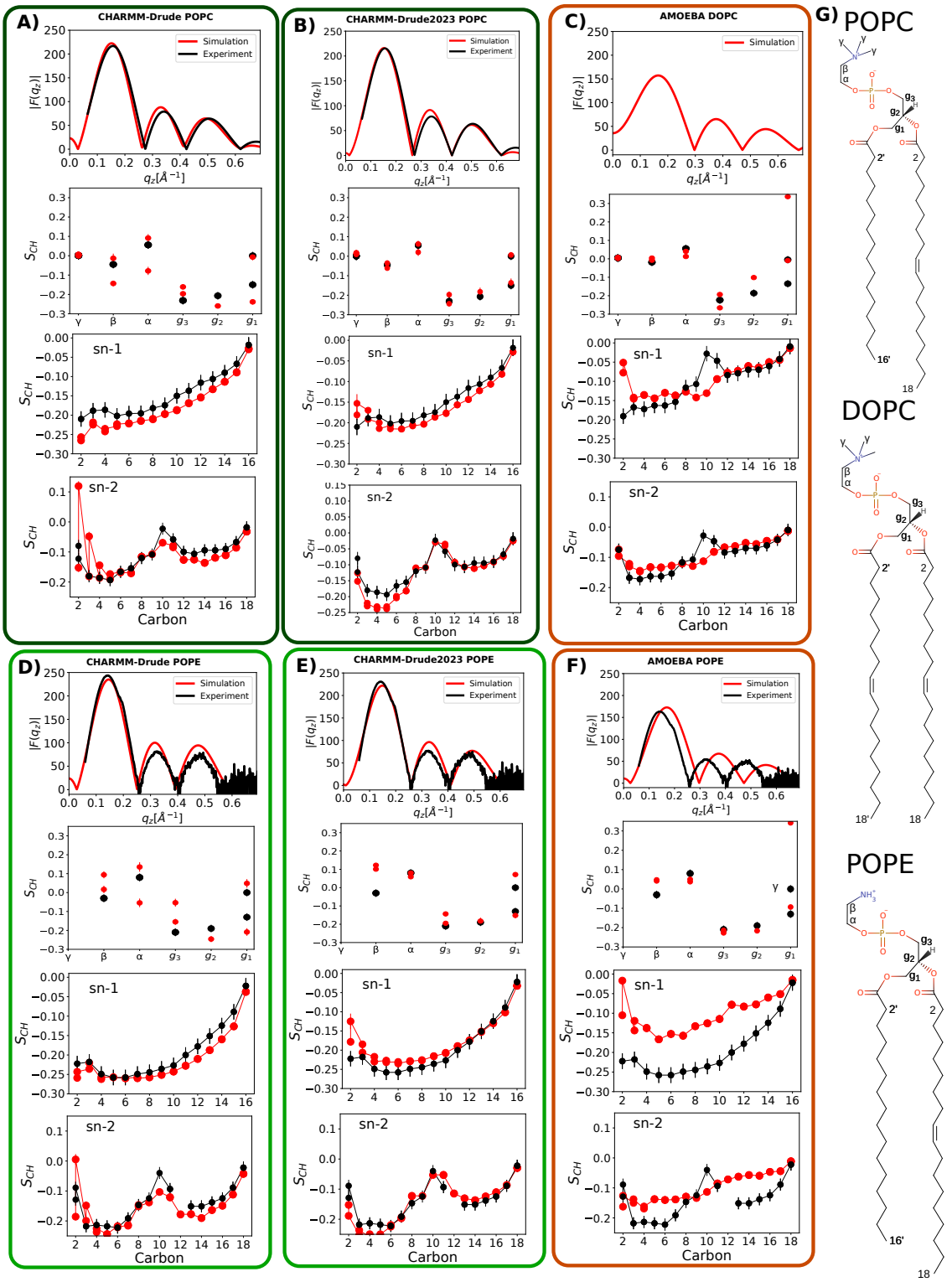

Figure 2: X-ray scattering form factors, and C-H bond order parameters for headgroup and glycerol backbone, and acyl chains (from top to bottom) compared between simulations and experiments using the NMRlipids databank. The atom labelling is as depicted in Fig. 1. Experimental data in this figure are originally reported in Refs. 29,32,42–44. For CHARMM-Drude2023 simulations we selected representative replicas among three available simulations, for example for differences between replicas for POPC see Fig. 6.

Table 1: NMRlipids databank quality metrics[32] and area per lipids (APL) compared between the best simulations found from the NMRlipids databank (OPLS3e[35] for POPC and GROMOS-CKP[36–38] for POPE), simulations with CHARMM36 force field, and simulations with polarizable force fields. Order parameter quality measures, $P^{\text{headgroup}}$, P^{sn-1}, and P^{sn-2}, present the average probability of order parameters within a given segment to agree with experiments (larger probabilities mean higher quality). Form factor quality measure, FF_q, presents the difference in essential features between simulated and experimental form factors (smaller values indicate higher quality). Experimental estimations for areas per lipid are POPC: 64.3±1Å^2,[39] DOPC: 67.5±1Å^2,[40] and POPE: 56.7±3Å^2.[41]

Lipid	Force field	$P^{\text{headgroup}}$	P^{sn-1}	P^{sn-2}	FF_q	APL
POPC	OPLS3e	0.76	0.87	0.85	0.15	66.5
POPC	CHARMM36	0.70	0.54	0.69	1.16	65.0
POPC	CHARMM-Drude2017	0.52	0.29	0.53	1.06	62.5
POPC	CHARMM-Drude2023	0.63	0.60	0.57	0.96	64.5
POPE	GROMOS-CKP	0.29	0.83	0.48	0.40	59.6
POPE	CHARMM36	0.54	0.52	0.27	1.30	57.2
POPE	CHARMM-Drude2017	0.06	0.53	0.27	0.80	56.6
POPE	CHARMM-Drude2023	0.28	0.59	0.54	0.00	61.4
POPE	AMOEBA	0.21	0.10	0.23	3.80	66.9
DOPC	AMOEBA	0.60	0.60	0.54	-	70.2

membrane data presented in the recent publication for the AMOEBA cholesterol model.[46] The unsatisfactory description of the lipid tail region and the area per lipid is further reflected in the inability of AMOEBA to capture the SAXS curves. Thus, we can conclude that our simulations with the AMOEBA parameters did not reproduce essential membrane properties.

Evaluation of conformational dynamics of lipids

C-H bond order parameters are sensitive to the conformational ensemble but the correspondence is not unique. Instead, they essentially describe the average of the distributions and do not contain information of the dynamics of the conformational sampling. Therefore, a simulation that reproduces the order parameters has an ensemble that is only potentially correct, and even the correct ensemble may not have the experimentally observed dynamics. To further elucidate this aspect in the case of polarizable force fields, we compared

NMR ^{13}C spin relaxation R_1 rates and C-H bond effective correlation times τ_{eff} with experiments[33] and best non-polarizable simulations from our previous study[30] for simulations with PC headgroups and the glycerol backbone in Fig. 3. This focus was chosen based on the availability of both experimental data and polarizable simulations. R_1 rates measured with typical magnetic field strengths are sensitive to rotational dynamics of C-H bonds with the timescales around ∼0.1-1 ns, while effective correlation times respond to a larger range of dynamical processes up to ∼1000 ns.[33] The effective correlation time can be interpreted as an average measure for how fast molecular conformations sample the phase space that leads to the average order parameters.

The effective correlation times in CHARMM-Drude2017 and CHARMM-Drude2023 simulations are approximately two and one orders of magnitude slower, respectively, than the values suggested by experiments and best available simulations (Fig. 3). This indicates that not only are the simulations with this polarizable force field computationally costlier for equivalent lengths of trajectory, but one would also have to simulate longer to obtain converged results. The non-polarizable counterpart of the Drude models, CHARMM36, exhibits much more realistic, faster effective correlation times. Also the dynamics in the fast range (R_1 rates), are on average slightly more realistic in the non-polarizable CHARMM36 compared to both of the polarizable counterparts. Interestingly, CHARMM-Drude models have been reported to have slower water hydrogen bonding dynamics around amino acids compared to their non-polarizable counterpart,[47] which might align with an overall slower dynamics of the model in addition to enhanced water binding.

In contrast to the Drude-based models investigated here, the R_1 spin relaxation times and effective correlation times from DOPC simulations with AMOEBA force field are close to experimental data from POPC and on par with the best non-polarizable models (Slipids and CHARMM36). The small difference in acyl chain composition (DOPC vs. POPC) is not expected to strongly affect headgroup dynamics due to effective decoupling between hydrophilic and hydrophobic membrane regions.[48,49]

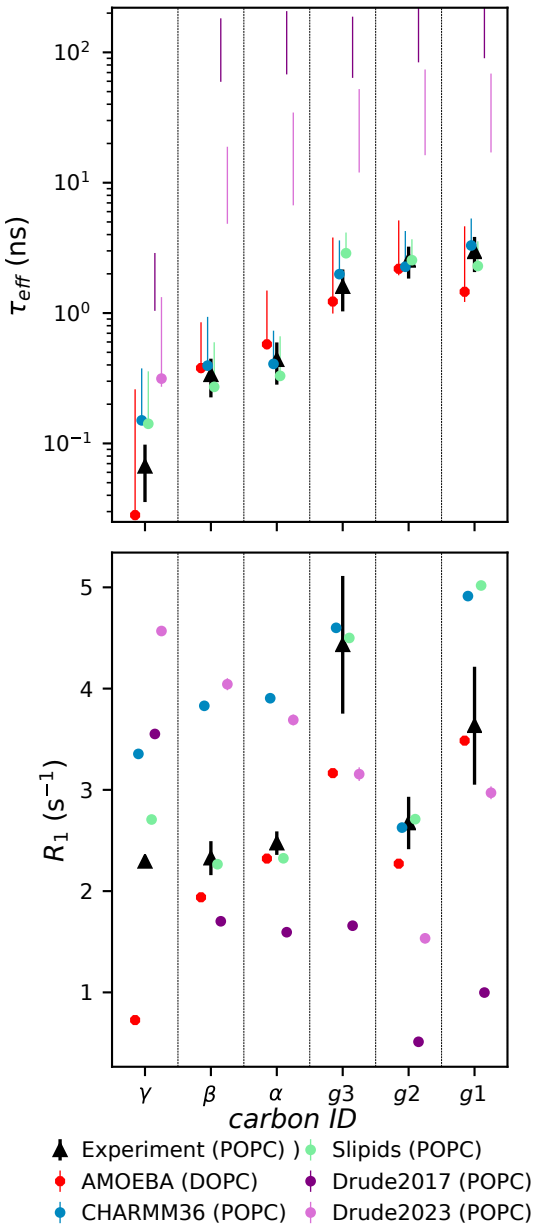

Figure 3: Effective correlation times (top) and R_1 rates (bottom) for the polarizable models and best performing non-polarizable force fields. Note, top panel axis is logarithmic to visualize the slow Drude dynamics. Experimental values are obtained from Ref. 48. All simulations used here were salt free.

Cation binding to membranes in polarizable simulations

Given the abundance of cations in biological systems, accurately capturing their interactions with membranes has the uttermost importance in MD simulations. A wealth of experimental evidence shows that monovalent ions (except for lithium) exhibit very weak binding affinity

of PC lipid bilayers, while multivalent ions like calcium bind more strongly.[27] However, simulations with non-polarizable force fields without any additional corrections systematically overestimate cation binding to lipid bilayers.[27] Implicit inclusion of electronic continuum correction (ECC) to both ion and lipid parameters can substantially improve the situation,[17,18,29] suggesting that electronic polarizability plays an important role in ion binding to membranes, which might further lead one to expect that simulations with polarizable force fields will perform better in this aspect and more accurately describe ion binding to membranes. To test this notion, we evaluated ion binding to membranes against the experimental NMR data using the "lipid electrometer," which involves quantifing the amount of ion binding to the membrane by monitoring the change in lipid headgroup order parameters in response to increasing salt concentration.[27] Changes in these order parameters induced by increasing NaCl or $CaCl_2$ concentration are shown in Fig. 4 for simulations and experiments, whereas Fig. 5 shows the density profiles of ions with respect to the bilayer normal. Results from AMBER-based ECC-lipid model are shown for the reference that gives a good agreement with experiments for cation binding.[17] We also show data from the non-polarizable CHARMM36 where NBFIX correction for the ion models was specifically developed to address overbinding.[50,51]

The CHARMM-Drude2017 predicts similar calcium ion density profile to ECC-lipids, in good agreement with experiments. However, the sodium binding is equally strong in these simulations in contrast with the experimental evidence.[27] Furthermore, the response of headgroup order parameters to the bound ions is not in qualitative agreement with experiments for CHARMM-Drude2017 simulations in Fig. 4. Particularly, increasing α carbon order parameters and forking upon ion binding are not observed in experiments. This is in contrast with the results from previous bechmarking of non-polarizable simulations,[27] where experimentally observed decrease of order parameters to more negative values upon ion binding were observed in all simulations, even though the binding affinity was often inaccurately predicted. This qualitative discrepancy in CHARMM-Drude2017 simulations most likely results

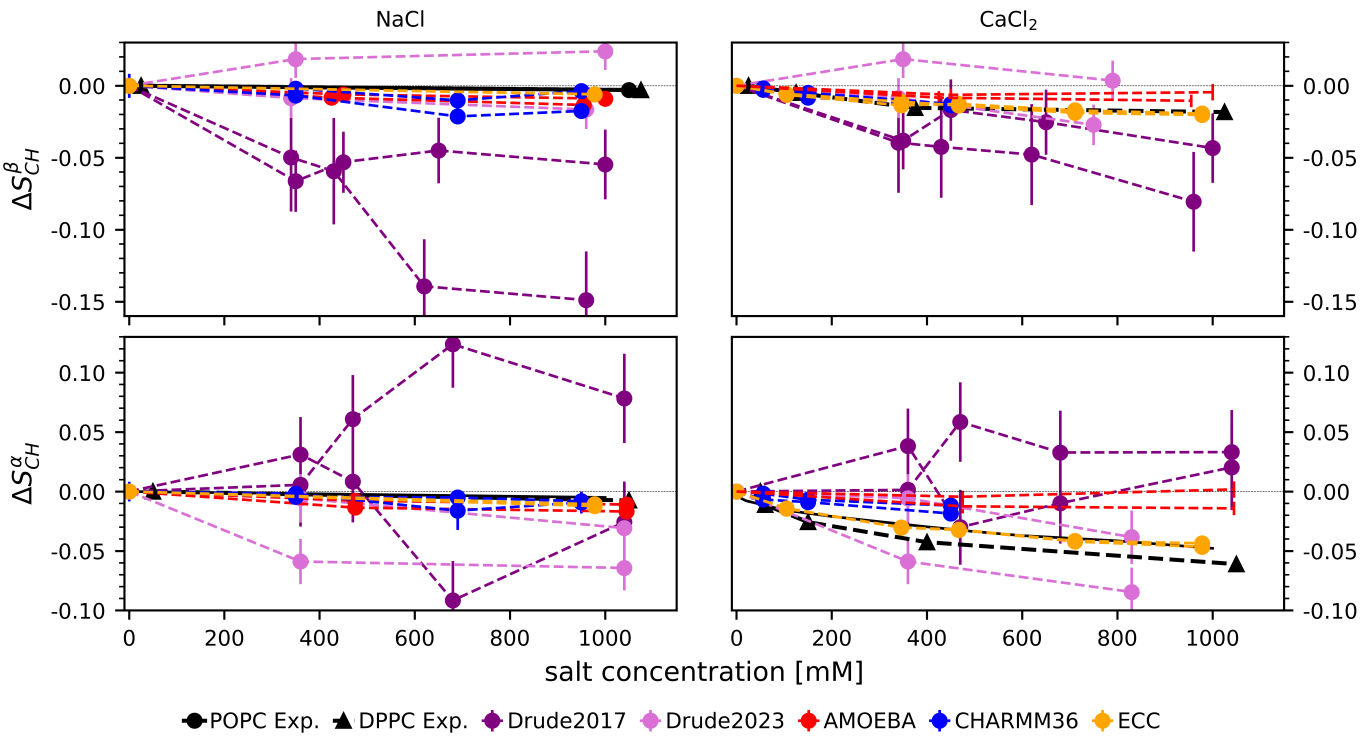

Figure 4: The change in the lipid head group order parameters β (top row) α (bottom row) upon increasing ion concentration with respect to the simulations without salt. CHARMM36 and ECC data is reproduced using the Zenodo repositories Ref.[52–55] and Ref.,[56] respectively.

from incorrect lipid headgroup conformational ensemble (see previous sections), which leads to inaccuracies in the structural response of the ensemble to ion binding. Excessive sodium binding in the CHARMM-Drude model has been observed before for systems containing peptides or amino acids[47,57] and deep-eutectic solvents.[58]

In simulations with CHARMM-Drude2023 parameters, sodium and calcium ion binding are in line with ECC-lipid simulations when comparing density profiles, although calcium binding affinity is slightly larger, ions penetrate deeper into the bilayer, and there is a stronger formation of ionic double layer by subsequent attraction of chloride into the bilayer in CHARMM-Drude2023 when compared with ECC-lipids. However, sodium or calcium ion binding seems to induce forking of lipid headgroup order parameters in CHARMM-Drude2023 simulations in contrast to experiments. This might indicate inaccurate structural response to ion binding, but poor convergence of the simulations owing to the slow confor-

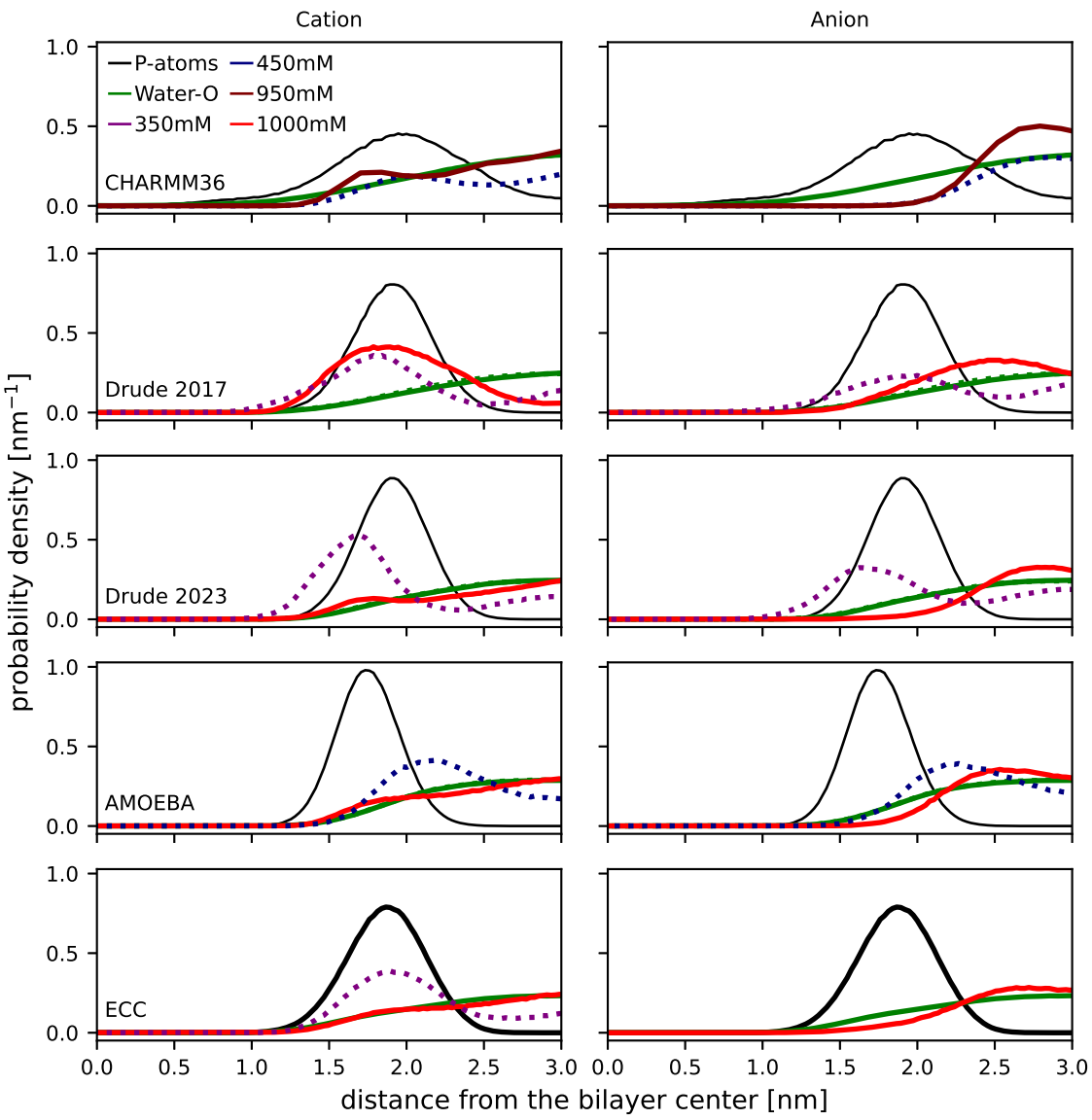

Figure 5: Density profiles along the membrane normal for the CHARMM36 (first row),[27] Drude 2017 and 2023 POPC (second and third rows), AMOEBA DOPC (fourth row), and electronic continuum correction (ECC, last row).[17] Solid and dashed lines are for the systems with the NaCl and $CaCl_2$, respectively. Please note that only 350 mM and 450 mM $CaCl_2$ concentrations are shown for the Drude and AMOEBA force fields, respectively, while 1000 mM NaCl concentration is shown for all force fields. CHARMM36 NaCl simulations are at 950 mM. CHARMM36 data is reproduced using the Zenodo repositories Ref.[52–55]

mational dynamics detected above cannot be ruled out in this case or in the case of the older 2017 version.

In AMOEBA simulations, sodium binds weakly and does not affect order parameters,

consistent with experiments and ECC-lipid simulations. Calcium binding affinity is similar to ECC-lipids, but order parameters also do not change upon binding contrasting the experiments. This can be explained by the binding position of calcium, which is outside phosphate density peak in AMOEBA simulations. In other simulations calcium penetrates to phosphate region or deeper and reorients the headgroup dipole, giving rise to changes in order parameters in line with the experimental data.[27]

In conclusion, incorporating explicit polarizability as implemented in CHARMM-Drude or AMOEBA parameters used here do not necessarily lead to improved description of cation binding to phospolipid membranes. However, these parameters do not correctly capture the response of lipid headgroup to cation binding to membrane, which most likely arises from inaccuracies in lipid parameters. Because such inaccuracies can also affect ion binding, it is difficult to isolate the explicit influence of polarizability per se on ion binding based on the results presented here. Nevertheless, CHARMM-Drude2023 predicts higher affinity for calcium than for sodium, which is in line with the wide range of experimental data.[27] This is a major improvement to non-polarizable CHARMM36 and CHARMM-Drude2017 which predict approximately similar binding to these ions in contrast to experiments.

Conclusions

Including electronic polarizability to MD simulation models of membranes is expected to improve the description of bilayer polar regions. However, performance of membrane simulations have not been evaluated with equal footing with non-polarizable membranes. Here, we used the quality evaluation metrics defined in the NMRlipids databank[32] together with additional analyzes on dynamics and ion binding to evaluate quality of two available polarizable lipid parameters, CHARMM-Drude[13,20] and AMOEBA,[14,21] against experimental data and results from the best-performing non-polarizable force fields. Considering the complexity and cost of simulations with polarizable models, it is crucial to understand their accuracy with respect to experiments and best non-polarizable models when planning simulations or

evaluating the reliability of simulation results.

Our comparisons of lipid conformations and dynamics revealed room for improvement in current polarizable parameters to reach the level of the best currently available non-polarizable parameters. CHARMM36-Drude models predict slightly too ordered membrane and struggle to correctly capture headgroup conformations and dynamics. The former issue is present also in non-polarizable CHARMM36, while slow headgroup dynamics and incorrect response to ion binding is present only in polarizable CHARMM36-Drude simulations. The tested AMOEBA parameters have difficulties to capture membrane ordering in acyl chain region, yet the PC and PE headgroup properties have similar or almost simular quality than the best non-polarizable force fields.

Sodium and calcium binding to membranes were evaluated against headgroup order parameter changes upon addition of NaCl or $CaCl_2$ in experiments and also compared with the ECClipids model with implicitly included electronic polarizability that currently gives the most accurate representation of ion binding against experiments. CHARMM-drude2023 model exhibits a major improvement to non-polarizable CHARMM and CHARMM-Drude2017 parameters as it correctly reproduces the stronger calcium binding with respect to sodium that was not present in older parameters. This difference between sodium and calcium binding is also present in simulations with AMOEBA parameters. However, calcium binding depth, affinity, and the consequent structural response of the lipids do not exactly align with experiments or ECClipids results neither in CHARMM-Drude2023 nor AMOEBA simulations. The incorrect response to ion binding likely connects to the other discussed inaccuracies related to lipid conformational ensembles, dynamics and membrane order.

In summary, the full potential and promise of explicitly polarizable lipid force fields to improve the description of polar membrane regions have not yet been fully realized. However, it seems likely that this is not due to implementation of polarizability, but rather arises from compatibility of other parameters, suchs as dihedral and Lennart-Jones, with polarizable electrons. Due to long history in developing these parameters for non-polarizable force fields,

it is not surprising that they out-perform their polarizable counterparts in many respects, as we here show for the case of certain phospholipid bilayers. On the other hand, improvements from CHARMM-Drude2017 to CHARMM-Drude2023 demonstrate the potential for tuning these parameters to improve polarizable force fields. Such endeavors are expected to substantially ease with emerging automized methods for parameter development.[20,31]

Methods

Using a polarizable force field for membrane simulations

While non-polarizable MD simulations of membranes can be nowadays routinely performed with several simulation packages and force fields, polarizable simulations bear many practical complications. Regarding currently popular MD simulation packages for membrane simulations, OpenMM supports both AMOEBA and Drude force fields, NAMD can only run the Drude force field whereas, GROMACS only has limited support for the Drude polarizable force field via an unofficial Git-branch.[59] TINKER is widely used with AMOEBA, but it does not support semi-isotropic pressure coupling, which is required in membrane simulations.[?] Therefore, we have selected to use OpenMM in all simulations in this work. CHARMM-GUI can generate the topology and input parameters for the Drude force field, which greatly simplifies the employment of this model in particular.[60] Standard protocols for AMOEBA lipid parameters are not available, but some parameters are available online.[9,61]

Another practical issue to be considered in polarizable membrane simulations is the increased computational cost arising from increased level of details obtained by explicit treatment of electronic polarizability. For the Drude-based models, this slowdown occurs both because the addition of the Drude particles increases the number of interaction pairs and the employed extended dual-Langevin thermostat requires a shorter 1 fs integration time step, compared to the 2 fs typically used for non-polarizable membrane simulations. The AMOEBA force field can use a multi time-step integration algorithm where the non-

electronic interactions are iterated with a 2 fs time step whereas more computationally unstable polarization terms are iterated with a smaller time step. However, the multi-time step scheme only partly mitigates the computational cost: one typically experiences almost a ten-fold decrease in the simulation speed while using the polarizable force fields.

All simulations performed in this work are listed in Table 2 with links to the openly available trajectory data. Data not mentioned here was obtained by analysing pre-existing trajectories from the NMRlipids databank.

Simulations with CHARMM-Drude parameters

CHARMM-Drude2017 simulations were performed with OpenMM 7.5.0[62] using parameters extracted with *Membrane Builder*[63–66] and *Drude Prepper*[60] from CHARMM-GUI.[67,68] Before starting the simulations, membrane structures were equilibrated for 200 ns using the non-polarizable CHARMM36 force field,[69] and the last frames of these simulations were used to generate the starting structures for the polarizable force field simulations.

CHARMM-Drude2023 force field parameters are currently not integrated into CHARMM-GUI. Therefore, the simulation setups with NaCl and $CaCl_2$ have been generated following the instructions in the original CHARMM-Drude2023 paper[20] using CHARMM program[70] and the last frame of 200 ns long CHARMM36 simulations (same as used for CHARMM-Drude2017). CHARMM-Drude2023 simulations without any ions have been directly obtained from Zenodo.[71,72]

A dual Langevin thermostat was employed to keep the Drude particles and the rest of the system at 1.0 K and 303 K, respectively. A Drude-hardwall of 0.02 nm was utilized to keep the Drude particles close to their parent atoms. Semi-isotropic Monte Carlo barostat was used to couple pressure to 1 bar independently in membrane plane and normal directions. Bonds containing the hydrogens were constrained. For CHARMM-Drude2017, particle mesh Ewald was used to compute the Coulomb interactions. Van der Waals interactions have been cut to 0 between 1.0 nm and 1.2 nm using a switching function. For the CHARMM-Drude2023,

Lennard-Jones particle-mesh Ewald (LJ-PME) method was used to compute the long-range dispersions.[73] Simulation frames have been saved in every 10 ps.

Simulations with AMOEBA parameters

AMOEBA force field parameters for OpenMM were obtained from GitHub.[9,61] All AMOEBA simulations have been run on OpenMM 7.1.1.[62] The same initial structures as the CHARMM-Drude simulations have been used to create the simulation setups. A multi-time step Langevin integrator was used to iterate the bonded and non-bonded interactions in every 0.5 fs and 2.0 fs, respectively. A non-bonded cutoff of 1.2 nm has been applied while semi-isotropic Monte Carlo barostat was used to couple pressure to 1 bar independently in membrane plane and normal directions. Simulation frames have been saved in every 10 ps. Further simulations details can be found in the input files of the respective simulations (Table 2)

Analysis of simulations

All simulations were first uploaded to the NMRlipids databank.[32] Area per lipids, X-ray scattering form factors, and order parameters (S_{CH}) are automatically calculated by the NMRLipids Databank[32] and were extracted from therein. Quality evaluation metrics were quantified as detailed in the NMRlipids databank[32] with the exception that POPC simulations at 303 K were coupled with the experimental data measured at 300 K, while in the NMRlipids databank simulations are coupled to experiments with the maximum temperature difference of two degrees. Shortly, order parameter qualities, $P^{\text{headgroup}}$, P^{sn-1}, and P^{sn-2}, presents an average probability for order parameters of a given segment to locate within experimental values, taking the error bars of both values into the account. Qualities of SAXS form factors, FF_q, are measured from the distance between first form factor minimum in simulated vs. experimental curve to avoid the effects from the simulation size dependency of the SAXS data. Note that in quantifying the bilayer electron densities for

calculation of SAXS curves the NMRlipids databank analysis algorithm places electrons as point charges at the atom centers without considering redistribution of charge density due to the polarizability. Nevertheless, we expect that this approximation does not have significant effect on the resulting SAXS form factors.

The R_1 rates and effective correlation times, along with the accompanying error estimates, are quantified from the trajectories as elaborated in Ref. 30. In-house python script available at XXX was used for this purpose. Source codes for all scripts and a detailed methodological explanation of the computed values are available in the referenced cited herein.

Table 2: Systems simulated for this work. Column N_l gives the number of lipids, N_w gives the number of water molecules, T(K) denotes the temperature in kelvins. Simulated time is listed in column t_{sim} and time used for analysis in $t_{analysis}$. Column "files" gives the reference to open access simulation data. The salt concentrations calculated as [salt]=N_c×[water] / N_w, where [water] = 55.5 M

Lipid/ion	force field	Ion (M)	N_l	N_w	N_{ion}	T (K)	t_{sim} (ns)	$t_{analysis}$ (ns)	files
POPC	Drude2017	0	144	6400	0	303	500	400	[74]
	Drude2023	0	72	2239	0	303	300	200	[72,75]
POPE	Drude2017	0	144	6400	0	308.15	350	300	[76]
	Drude2023	0	72	2304	0	303	300	200	[71,77]
	AMOEBA	0	72	2880	0	303	305.94	305.94	[78]
POPC:NaCl	Drude2017	0.350	144	6400	41	303	500	400	[79]
	Drude2017	0.450	144	6400	51	303	500	400	[80]
	Drude2017	0.650	144	6400	77	303	500	400	[81]
	Drude2017	1.0	144	6400	115	303	500	400	[82]
	Drude2023	1.0	128	6400	41	303	223.97	220.14	[83]
	Drude2023	1.0	128	6400	115	303	220.14	220.14	[84]
POPC:$CaCl_2$	Drude2017	0.350	144	6400	41	303	500	400	[85]
	Drude2017	0.450	144	6400	52	303	500	400	[86]
	Drude2017	0.650	144	6400	76	303	500	400	[87]
	Drude2017	1.0	144	6400	114	303	500	400	[88]
	Drude2023	0.350	128	6400	41	303	219.59	219.59	[89]
	Drude2023	0.790	128	6400	91	303	214.85	214.85	[90]
DOPC	AMOEBA	0	72	2880	0	303	201.61	201.61	[91]
DOPC:NaCl	AMOEBA	0.450	72	2880	17	303	218.41	218.41	[92]
	AMOEBA	1.0	72	2880	35	303	201.61	201.61	[93]
DOPC:$CaCl_2$	AMOEBA	0.450	72	2880	16	303	218.41	218.41	[94]
	AMOEBA	1.0	72	2880	36	303	218.41	218.41	[95]

1.check the simualation settings (especially the temperature

Acknowledgement

J.J.M. thanks Huiying Chu (from the Li lab) for technical discussions and Sameer Varma for useful suggestions.

Supporting Information Available

References

(1) Thole, B. Molecular polarizabilities calculated with a modified dipole interaction. *Chemical Physics* **1981**, *59*, 341–350.

(2) Ando, K. A stable fluctuating-charge polarizable model for molecular dynamics simulations: Application to aqueous electron transfers. *The Journal of Chemical Physics* **2001**, *115*, 5228–5237.

(3) Grossfield, A.; Ren, P.; Ponder, J. W. Ion Solvation Thermodynamics from Simulation with a Polarizable Force Field. *Journal of the American Chemical Society* **2003**, *125*, 15671–15682, PMID: 14664617.

(4) Lamoureux, G.; Roux, B. Modeling induced polarization with classical Drude oscillators: Theory and molecular dynamics simulation algorithm. *The Journal of Chemical Physics* **2003**, *119*, 3025–3039.

(5) Lemkul, J. A.; Huang, J.; Roux, B.; MacKerell, A. D. J. An Empirical Polarizable Force Field Based on the Classical Drude Oscillator Model: Development History and Recent Applications. *Chemical Reviews* **2016**, *116*, 4983–5013, PMID: 26815602.

(6) Baker, C. M. Polarizable force fields for molecular dynamics simulations of biomolecules. *Wiley Interdisciplinary Reviews: Computational Molecular Science* **2015**, *5*, 241–254.

(7) Inakollu, V. S.; Geerke, D. P.; Rowley, C. N.; Yu, H. Polarisable force fields: what do they add in biomolecular simulations? *Current Opinion in Structural Biology* **2020**, *61*, 182–190.

(8) Roux, B.; Bernèche, S.; Egwolf, B.; Lev, B.; Noskov, S. Y.; Rowley, C. N.; Yu, H.

Ion selectivity in channels and transporters. *Journal of general physiology* **2011**, *137*, 415–426.

(9) Klesse, G.; Rao, S.; Tucker, S. J.; Sansom, M. S. Induced polarization in molecular dynamics simulations of the 5-HT3 receptor channel. *Journal of the American Chemical Society* **2020**, *142*, 9415–9427.

(10) Prajapati, J. D.; Mele, C.; Aksoyoglu, M. A.; Winterhalter, M.; Kleinekathöfer, U. Computational modeling of ion transport in bulk and through a nanopore using the drude polarizable force field. *Journal of Chemical Information and Modeling* **2020**, *60*, 3188–3203.

(11)

(12) Salsbury, A. M.; Michel, H. M.; Lemkul, J. A. Ion-Dependent Conformational Plasticity of Telomeric G-Hairpins and G-Quadruplexes. *ACS Omega* **2022**, *7*, 23368–23379.

(13) Li, H.; Chowdhary, J.; Huang, L.; He, X.; MacKerell Jr, A. D.; Roux, B. Drude polarizable force field for molecular dynamics simulations of saturated and unsaturated zwitterionic lipids. *Journal of chemical theory and computation* **2017**, *13*, 4535–4552.

(14) Chu, H.; Peng, X.; Li, Y.; Zhang, Y.; Li, G. A polarizable atomic multipole-based force field for molecular dynamics simulations of anionic lipids. *Molecules* **2018**, *23*, 77.

(15) Lynch, C. I.; Klesse, G.; Rao, S.; Tucker, S. J.; Sansom, M. S. P. Water Nanoconfined in a Hydrophobic Pore: Molecular Dynamics Simulations of Transmembrane Protein 175 and the Influence of Water Models. *ACS Nano* **2021**, *15*, 19098–19108, PMID: 34784172.

(16) Chen, P.; Vorobyov, I.; Roux, B.; Allen, T. W. Molecular Dynamics Simulations Based on Polarizable Models Show that Ion Permeation Interconverts between Different Mech-

anisms as a Function of Membrane Thickness. *The Journal of Physical Chemistry B* **2021**, *125*, 1020–1035, PMID: 33493394.

(17) Melcr, J.; Martinez-Seara, H.; Nencini, R.; Kolafa, J.; Jungwirth, P.; Ollila, O. H. S. Accurate Binding of Sodium and Calcium to a POPC Bilayer by Effective Inclusion of Electronic Polarization. *J. Phys. Chem. B* **2018**, *122*, 4546–4557.

(18) Melcr, J.; Ferreira, T. M.; Jungwirth, P.; Ollila, O. S. Improved Cation Binding to Lipid Bilayers with Negatively Charged POPS by Effective Inclusion of Electronic Polarization. *Journal of chemical theory and computation* **2019**,

(19) Nencini, R.; Ollila, O. H. S. Charged Small Molecule Binding to Membranes in MD Simulations Evaluated against NMR Experiments. *The Journal of Physical Chemistry B* **2022**, *126*, 6955–6963.

(20) Yu, Y.; Venable, R. M.; Thirman, J.; Chatterjee, P.; Kumar, A.; Pastor, R. W.; Roux, B.; MacKerell Jr, A. D.; Klauda, J. B. Drude Polarizable Lipid Force Field with Explicit Treatment of Long-Range Dispersion: Parametrization and Validation for Saturated and Monounsaturated Zwitterionic Lipids. *Journal of Chemical Theory and Computation* **2023**, *19*, 2590–2605.

(21) Chu, H.; Peng, X.; Li, Y.; Zhang, Y.; Min, H.; Li, G. Polarizable atomic multipole-based force field for DOPC and POPE membrane lipids. *Molecular Physics* **2018**, *116*, 1037–1050.

(22) Lucas, T. R.; Bauer, B. A.; Patel, S. Charge equilibration force fields for molecular dynamics simulations of lipids, bilayers, and integral membrane protein systems. *Biochimica et Biophysica Acta (BBA)-Biomembranes* **2012**, *1818*, 318–329.

(23) Ponder, J. W.; Wu, C.; Ren, P.; Pande, V. S.; Chodera, J. D.; Schnieders, M. J.; Haque, I.; Mobley, D. L.; Lambrecht, D. S.; DiStasio Jr, R. A., et al. Current status of

the AMOEBA polarizable force field. *The journal of physical chemistry B* **2010**, *114*, 2549–2564.

(24) Patel, S.; Brooks III, C. L. CHARMM fluctuating charge force field for proteins: I parameterization and application to bulk organic liquid simulations. *Journal of computational chemistry* **2004**, *25*, 1–16.

(25) Duboué-Dijon, E.; Javanainen, M.; Delcroix, P.; Jungwirth, P.; Martinez-Seara, H. A practical guide to biologically relevant molecular simulations with charge scaling for electronic polarization. *The Journal of Chemical Physics* **2020**, *153*, 050901.

(26) Botan, A. et al. Toward Atomistic Resolution Structure of Phosphatidylcholine Headgroup and Glycerol Backbone at Different Ambient Conditions. *The Journal of Physical Chemistry B* **2015**, *119*, 15075–15088, PMID: 26509669.

(27) Catte, A.; Girych, M.; Javanainen, M.; Loison, C.; Melcr, J.; Miettinen, M. S.; Monticelli, L.; Määttä, J.; Oganesyan, V. S.; Ollila, O. H. S.; Tynkkynen, J.; Vilov, S. Molecular electrometer and binding of cations to phospholipid bilayers. *Phys. Chem. Chem. Phys.* **2016**, *18*, 32560–32569.

(28) Antila, H.; Buslaev, P.; Favela-Rosales, F.; Ferreira, T. M.; Gushchin, I.; Javanainen, M.; Kav, B.; Madsen, J. J.; Melcr, J.; Miettinen, M. S.; Määttä, J.; Nencini, R.; Ollila, O. H. S.; Piggot, T. J. Headgroup Structure and Cation Binding in Phosphatidylserine Lipid Bilayers. *The Journal of Physical Chemistry B* **2019**, *123*, 9066–9079, PMID: 31574222.

(29) Bacle, A. et al. Inverse Conformational Selection in Lipid–Protein Binding. *Journal of the American Chemical Society* **2021**, *143*, 13701–13709.

(30) Antila, H. S.; M. Ferreira, T.; Ollila, O. H. S.; Miettinen, M. S. Using Open Data to Rapidly Benchmark Biomolecular Simulations: Phospholipid Conformational Dy-

namics. *Journal of Chemical Information and Modeling* **2021**, *61*, 938–949, PMID: 33496579.

(31) Antila, H. S.; Kav, B.; Miettinen, M. S.; Martinez-Seara, H.; Jungwirth, P.; Ollila, O. H. S. Emerging Era of Biomolecular Membrane Simulations: Automated Physically-Justified Force Field Development and Quality-Evaluated Databanks. *The Journal of Physical Chemistry B* **2022**, *126*, 4169–4183.

(32) Kiirikki, A.; Antila, H.; Bort, L.; Buslaev, P.; Fernando, F.; Mendes Ferreira, T.; Fuchs, P.; Garcia-Fandino, R.; Gushchin, I.; Kav, B.; et al., NMRlipids Databank makes data-driven analysis of biomembrane properties accessible for all. *ChemRxiv* **2023**,

(33) Ferreira, T. M.; Ollila, O. H. S.; Pigliapochi, R.; Dabkowska, A. P.; Topgaard, D. Model-free estimation of the effective correlation time for C-H bond reorientation in amphiphilic bilayers: ^{1}H-^{13}C solid-state NMR and MD simulations. *J. Chem. Phys.* **2015**, *142*, 044905.

(34) Ollila, O. S.; Pabst, G. Atomistic resolution structure and dynamics of lipid bilayers in simulations and experiments. *Biochim. Biophys. Acta* **2016**, *1858*, 2512 – 2528.

(35) Roos, K.; Wu, C.; Damm, W.; Reboul, M.; Stevenson, J. M.; Lu, C.; Dahlgren, M. K.; Mondal, S.; Chen, W.; Wang, L.; Abel, R.; Friesner, R. A.; Harder, E. D. OPLS3e: Extending Force Field Coverage for Drug-Like Small Molecules. *Journal of Chemical Theory and Computation* **2019**, *15*, 1863–1874.

(36) Chandrasekhar, I.; Kastenholz, M.; Lins, R.; Oostenbrink, C.; Schuler, L.; Tieleman, D.; Gunsteren, W. A consistent potential energy parameter set for lipids: dipalmitoylphosphatidylcholine as a benchmark of the GROMOS96 45A3 force field. *Eur. Biophys. J.* **2003**, *32*, 67–77.

(37) Kukol, A. Lipid Models for United-Atom Molecular Dynamics Simulations of Proteins. *J. Chem. Theory Comput.* **2009**, *5*, 615–626.

(38) Piggot, T. J.; Piñeiro, Á.; Khalid, S. Molecular Dynamics Simulations of Phosphatidylcholine Membranes: A Comparative Force Field Study. *J. Chem. Theory Comput.* **2012**, *8*, 4593–4609.

(39) Kučerka, N.; Nieh, M.-P.; Katsaras, J. Fluid phase lipid areas and bilayer thicknesses of commonly used phosphatidylcholines as a function of temperature. *Biochimica et Biophysica Acta (BBA) - Biomembranes* **2011**, *1808*, 2761–2771.

(40) Kučerka, N.; Nagle, J. F.; Sachs, J. N.; Feller, S. E.; Pencer, J.; Jackson, A.; Katsaras, J. Lipid Bilayer Structure Determined by the Simultaneous Analysis of Neutron and X-Ray Scattering Data. *Biophysical Journal* **2008**, *95*, 2356–2367.

(41) Rickeard, B. W.; Nguyen, M. H. L.; DiPasquale, M.; Yip, C. G.; Baker, H.; Heberle, F. A.; Zuo, X.; Kelley, E. G.; Nagao, M.; Marquardt, D. Transverse lipid organization dictates bending fluctuations in model plasma membranes. *Nanoscale* **2020**, *12*, 1438–1447.

(42) Ferreira, T. M.; Coreta-Gomes, F.; Ollila, O. H. S.; Moreno, M. J.; Vaz, W. L. C.; Topgaard, D. Cholesterol and POPC segmental order parameters in lipid membranes: solid state ^{1}H-^{13}C NMR and MD simulation studies. *Phys. Chem. Chem. Phys.* **2013**, *15*, 1976–1989.

(43) Javanainen, M.; Heftberger, P.; Madsen, J. J.; Miettinen, M. S.; Pabst, G.; Ollila, O. H. S. Quantitative Comparison against Experiments Reveals Imperfections in Force Fields' Descriptions of POPC–Cholesterol Interactions. *Journal of Chemical Theory and Computation* **2023**, *19*, 6342–6352.

(44) Kučerka, N.; van Oosten, B.; Pan, J.; Heberle, F. A.; Harroun, T. A.; Katsaras, J. Molecular Structures of Fluid Phosphatidylethanolamine Bilayers Obtained from Simulation-to-Experiment Comparisons and Experimental Scattering Density Profiles. *The Journal of Physical Chemistry B* **2015**, *119*, 1947–1956.

(45) Ollila, S.; Hyvönen, M. T.; Vattulainen, I. Polyunsaturation in Lipid Membranes: Dynamic Properties and Lateral Pressure Profiles. *J. Phys. Chem. B* **2007**, *111*, 3139–3150.

(46) Li, Y.; Liu, Y.; Yang, B.; Li, G.; Chu, H. Polarizable atomic multipole-based force field for cholesterol. *Journal of Biomolecular Structure and Dynamics* **2023**, *0*, 1–11, PMID: 37565356.

(47) Ngo, V. A.; Fanning, J. K.; Noskov, S. Y. Comparative Analysis of Protein Hydration from MD simulations with Additive and Polarizable Force Fields. *Advanced Theory and Simulations* **2019**, *2*, 1800106.

(48) Antila, H. S.; Wurl, A.; Ollila, O. S.; Miettinen, M. S.; Ferreira, T. M. Rotational decoupling between the hydrophilic and hydrophobic regions in lipid membranes. *Biophysical Journal* **2022**, *121*, 68–78.

(49) Klauda, J. B.; Roberts, M. F.; Redfield, A. G.; Brooks, B. R.; Pastor, R. W. Rotation of Lipids in Membranes: Molecular Dynamics Simulation, 31P Spin-Lattice Relaxation, and Rigid-Body Dynamics. *Biophysical Journal* **2008**, *94*, 3074–3083.

(50) Venable, R. M.; Luo, Y.; Gawrisch, K.; Roux, B.; Pastor, R. W. Simulations of Anionic Lipid Membranes: Development of Interaction-Specific Ion Parameters and Validation Using NMR Data. *The Journal of Physical Chemistry B* **2013**, *117*, 10183–10192, PMID: 23924441.

(51) Han, K.; Venable, R. M.; Bryant, A.-M.; Legacy, C. J.; Shen, R.; Li, H.; Roux, B.; Gericke, A.; Pastor, R. W. Graph–Theoretic Analysis of Monomethyl Phosphate Clustering in Ionic Solutions. *The Journal of Physical Chemistry B* **2018**, *122*, 1484–1494, PMID: 29293344.

(52) Ollila, S. MD simulation trajectory and related files for POPC bilayer with 350mM NaCl (CHARMM36, Gromacs 4.5). 2015; `https://doi.org/10.5281/zenodo.32496`.

(53) Ollila, S. MD simulation trajectory and related files for POPC bilayer with 690mM NaCl (CHARMM36, Gromacs 4.5). 2015; https://doi.org/10.5281/zenodo.32497.

(54) Ollila, S. MD simulation trajectory and related files for POPC bilayer with 950mM NaCl (CHARMM36, Gromacs 4.5). 2015; https://doi.org/10.5281/zenodo.32498.

(55) Nencini, R. CHARMM36, NB-Fix approaches, without NBFIX, POPC membrane, Ca, Na ions,. 2019; https://doi.org/10.5281/zenodo.3434396.

(56) Melcr, J. Simulations of POPC lipid bilayer in water solution at various NaCl, KCl and CaCl2 concentrations using ECC-POPC force field. 2017; https://doi.org/10.5281/zenodo.3335503.

(57) Kav, B.; Strodel, B. Does the inclusion of electronic polarisability lead to a better modelling of peptide aggregation? *RSC Adv.* **2022**, *12*, 20829–20837.

(58) Shayestehpour, O.; Zahn, S. Ion Correlation in Choline Chloride–Urea Deep Eutectic Solvent (Reline) from Polarizable Molecular Dynamics Simulations. *The Journal of Physical Chemistry B* **2022**, *126*, 3439–3449.

(59)

(60) Kognole, A. A.; Lee, J.; Park, S.-J.; Jo, S.; Chatterjee, P.; Lemkul, J. A.; Huang, J.; MacKerell Jr, A. D.; Im, W. CHARMM-GUI Drude prepper for molecular dynamics simulation using the classical Drude polarizable force field. *Journal of computational chemistry* **2022**, *43*, 359–375.

(61) OpenMM Scripts for AMOEBA Force Field MD Simulations. https://github.com/Inniag/openmm-scripts-amoeba.

(62) Eastman, P.; Swails, J.; Chodera, J. D.; McGibbon, R. T.; Zhao, Y.; Beauchamp, K. A.; Wang, L.-P.; Simmonett, A. C.; Harrigan, M. P.; Stern, C. D., et al. OpenMM 7: Rapid

development of high performance algorithms for molecular dynamics. *PLoS computational biology* **2017**, *13*, e1005659.

(63) Wu, E. L.; Cheng, X.; Jo, S.; Rui, H.; Song, K. C.; Dávila-Contreras, E. M.; Qi, Y.; Lee, J.; Monje-Galvan, V.; Venable, R. M., et al. CHARMM-GUI membrane builder toward realistic biological membrane simulations. 2014.

(64) Jo, S.; Lim, J. B.; Klauda, J. B.; Im, W. CHARMM-GUI Membrane Builder for mixed bilayers and its application to yeast membranes. *Biophysical journal* **2009**, *97*, 50–58.

(65) Jo, S.; Kim, T.; Im, W. Automated builder and database of protein/membrane complexes for molecular dynamics simulations. *PloS one* **2007**, *2*, e880.

(66) Lee, J.; Patel, D. S.; Ståhle, J.; Park, S.-J.; Kern, N. R.; Kim, S.; Lee, J.; Cheng, X.; Valvano, M. A.; Holst, O., et al. CHARMM-GUI membrane builder for complex biological membrane simulations with glycolipids and lipoglycans. *Journal of chemical theory and computation* **2018**, *15*, 775–786.

(67) Jo, S.; Kim, T.; Iyer, V. G.; Im, W. CHARMM-GUI: a web-based graphical user interface for CHARMM. *Journal of computational chemistry* **2008**, *29*, 1859–1865.

(68) Lee, J.; Cheng, X.; Swails, J. M.; Yeom, M. S.; Eastman, P. K.; Lemkul, J. A.; Wei, S.; Buckner, J.; Jeong, J. C.; Qi, Y., et al. CHARMM-GUI input generator for NAMD, GROMACS, AMBER, OpenMM, and CHARMM/OpenMM simulations using the CHARMM36 additive force field. *Journal of chemical theory and computation* **2016**, *12*, 405–413.

(69) Klauda, J. B.; Venable, R. M.; Freites, J. A.; O'Connor, J. W.; Tobias, D. J.; Mondragon-Ramirez, C.; Vorobyov, I.; MacKerell Jr, A. D.; Pastor, R. W. Update of the CHARMM all-atom additive force field for lipids: validation on six lipid types. *The journal of physical chemistry B* **2010**, *114*, 7830–7843.

(70) Brooks, B. R.; Brooks III, C. L.; Mackerell Jr, A. D.; Nilsson, L.; Petrella, R. J.; Roux, B.; Won, Y.; Archontis, G.; Bartels, C.; Boresch, S., et al. CHARMM: the biomolecular simulation program. *Journal of computational chemistry* **2009**, *30*, 1545–1614.

(71) Venable, R. M. OpenMM simulations of POPE using the CHARMM Drude2023 force field. 2023; `https://doi.org/10.5281/zenodo.7872447`, The data files contain additional atom types for the Drude particles and oxygen lone pairs.

(72) Venable, R. M. OpenMM simulations of POPC using the CHARMM Drude2023 force field. 2023; `https://doi.org/10.5281/zenodo.7871949`, The data files contain additional atom types for the Drude particles and oxygen lone pairs.

(73) Wennberg, C. L.; Murtola, T.; Hess, B.; Lindahl, E. Lennard-Jones lattice summation in bilayer simulations has critical effects on surface tension and lipid properties. *Journal of chemical theory and computation* **2013**, *9*, 3527–3537.

(74) Kav, B. Pure POPC membrane simulations with the CHARMM- Drude force field (OpenMM 7.5.0). 2021; `https://doi.org/10.5281/zenodo.7607436`.

(75) Kav, B. OpenMM simulations of POPC using the CHARMM Drude2023 force field in xtc format. 2023; `https://doi.org/10.5281/zenodo.7916287`.

(76) Kav, B. Pure POPE membrane simulations with the CHARMM- Drude force field (OpenMM 7.5.0). 2021; `https://doi.org/10.5281/zenodo.7604627`.

(77) Kav, B. OpenMM simulations of POPE using the CHARMM Drude2023 force field in xtc format. 2023; `https://doi.org/10.5281/zenodo.7916494`.

(78) Kav, B. MD Simulation data for a pure POPE bilayer with AMOEBA force field + OpenMM. 2023; `https://doi.org/10.5281/zenodo.7622838`.

(79) Kav, B. Pure POPC Membrane with 350mM NaCl simulations using Drude Polarizable Force Field and OpenMM. 2020; https://doi.org/10.5281/zenodo.7586915.

(80) Kav, B. Pure POPC Membrane with 450mM NaCl simulations using Drude Polarizable Force Field and OpenMM. 2020; https://doi.org/10.5281/zenodo.7591753.

(81) Kav, B. Pure POPC Membrane with 650mM NaCl simulations using Drude Polarizable Force Field and OpenMM. 2020; https://doi.org/10.5281/zenodo.7596011.

(82) Kav, B. Pure POPC Membrane with 1000mM NaCl simulations using Drude Polarizable Force Field and OpenMM. 2020; https://doi.org/10.5281/zenodo.7600326.

(83) Kav, B. Pure POPC membrane simulations with 350 mM NaCl with the CHARMM-Drude2023 force field (OpenMM). 2023; https://doi.org/10.5281/zenodo.8000095.

(84) Kav, B. Pure POPC membrane simulations with 1000 mM NaCl with the CHARMM-Drude2023 force field (OpenMM). 2023; https://doi.org/10.5281/zenodo.8000133.

(85) Kav, B. Pure POPC Membrane with 350mM CaCl2 simulations using Drude Polarizable Force Field and OpenMM. 2020; https://doi.org/10.5281/zenodo.7600827.

(86) Kav, B. Pure POPC Membrane with 450mM CaCl2 simulations using Drude Polarizable Force Field and OpenMM. 2020; https://doi.org/10.5281/zenodo.7605016.

(87) Kav, B. Pure POPC Membrane with 650mM CaCl2 simulations using Drude Polarizable Force Field and OpenMM. 2020; https://doi.org/10.5281/zenodo.7604040.

(88) Kav, B. Pure POPC membrane simulations with 1000 mM CaCl2 with the CHARMM-Drude force field (OpenMM). 2023; https://doi.org/10.5281/zenodo.7658975.

(89) Kav, B. Pure POPC membrane simulations with 350 mM CaCl2 with the CHARMM-Drude2023 force field (OpenMM). 2023; https://doi.org/10.5281/zenodo.8000065.

(90) Kav, B. Pure POPC membrane simulations with 790 mM CaCl2 with the CHARMM-Drude2023 force field (OpenMM). 2023; https://doi.org/10.5281/zenodo.7992137.

(91) Kav, B. MD Simulation data for a pure DOPC bilayer without salt with AMOEBA force field + OpenMM. 2022; https://doi.org/10.5281/zenodo.7604681.

(92) Kav, B. MD Simulation data for a pure DOPC bilayer (450 mM NaCl) with AMOEBA force field + OpenMM. 2022; https://doi.org/10.5281/zenodo.7604711.

(93) Kav, B. MD Simulation data for a pure DOPC bilayer (1000 mM NaCl) with AMOEBA force field + OpenMM. 2023; https://doi.org/10.5281/zenodo.7625844.

(94) Kav, B. MD Simulation data for a pure DOPC bilayer (450 mM CaCl2) with AMOEBA force field + OpenMM. 2022; https://doi.org/10.5281/zenodo.7604842.

(95) Kav, B. MD Simulation data for a pure DOPC bilayer (1000 mM CaCl2) with AMOEBA force field + OpenMM. 2022; https://doi.org/10.5281/zenodo.7604810.

Supplementary figures

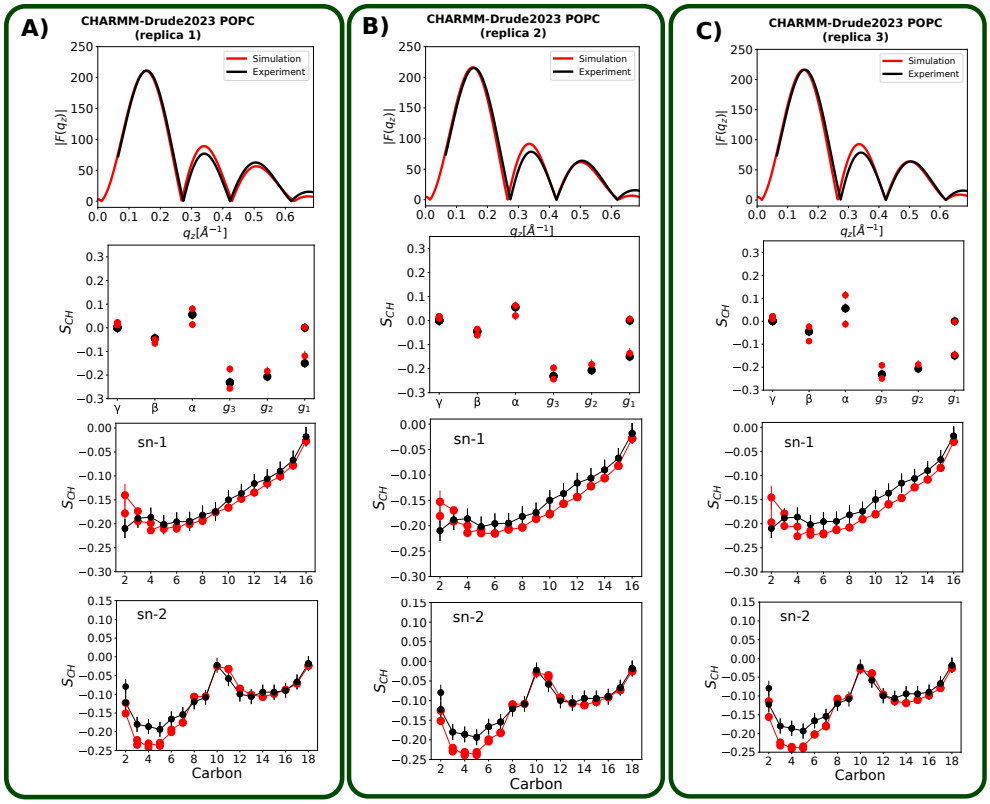

Figure 6: X-ray scattering form factors, and C-H bond order parameters for headgroup and glycerol backbone, and acyl chains (from top to bottom) compared between simulations and experiments using the NMRlipids databank. The atom labelling is as depicted in Fig. 1.

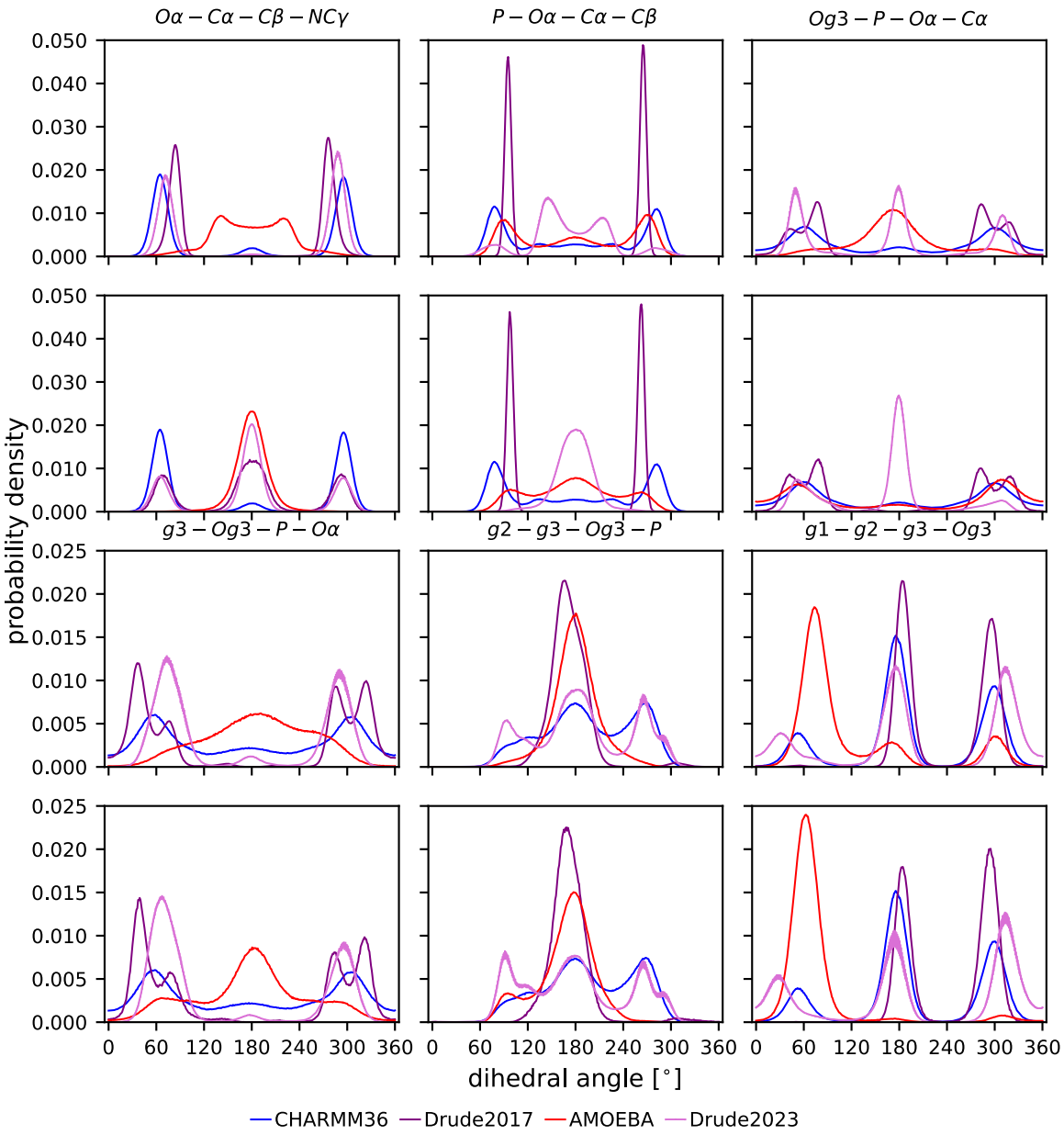

Figure 7: The distributions of the torsion angles for the head group atoms. For each torsion angle, the upper and lower rows contain the DOPC (AMOEBA) - POPC (Drude/Drude2023) and POPE lipids, respectively.